scientific reports

Check for updates

OPEN

Quantification of hounsfield unit difference in heterogeneous hematoma predicts poor functional outcomes in acute intracerebral hemorrhage

Qian Wu[1,4], Lei Huang[2,4], Na Chen[2], Siying Ren[1], Fei Ye[1], Xu Zhao[1], Guofeng Wu[1] & Likun Wang[1,2,3]✉

Heterogeneous hematoma exhibiting a blend sign undergo dynamic changes associated with neurological injury. This study quantified hyperdense and hypodense regions of blend sign on serial non-contrast computed tomography (NCCT) using ITK-SNAP, calculated the mean hounsfield unit (HU) difference (dHU), and evaluated its prognostic value in 261 patients with intracerebral hemorrhage (ICH). All patients underwent baseline CT within 6 h of symptom onset and follow-up CT within 24 h. Logistic regression and ROC analysis showed that a higher dHU was independently associated with secondary neurological deterioration, 30-day mortality, and poor 3-month functional outcomes. A dHU > 3.25 predicted poor prognosis with good specificity (AUC 0.707, $P < 0.001$). These findings suggest that the dHU of heterogeneous hematoma based on serial CT scans is independently associated with poor outcomes after acute ICH.

Trial registration: https://ClinicalTrials.gov, NCT05548530.

Keywords Intracerebral hemorrhage, Blend sign, Computed tomography, Difference of mean hounsfield units (dHU), Poor outcomes

Intracerebral hemorrhage (ICH), defined as bleeding within the brain resulting from blood vessel rupture independent of external factors, accounts for approximately 20–30% of all acute stroke cases[1]. The relative prevalence of ICH, however, is substantially higher in some populations. In the Chinese-American population for instance, ICH accounts for approximately 33% of acute strokes compared to only 12% among Caucasians[2]. Furthermore, ICH is one of the most lethal forms of acute stroke, with an early mortality rate estimated at 30–40%, and the disability-adjusted life years lost due to ICH is greater than that of ischemic stroke resulting from vessel occlusion. Survivors may also exhibit severe functional and cognitive impairments long after ICH onset[3].

Despite substantial advancements in recent years in elucidating pathological mechanisms and conducting clinical trials for ICH, effective interventions targeting post-hemorrhagic cascade injury remain limited in clinical practice. In this context, the early identification of patient populations at high risk of clinical deterioration has emerged as a critical strategy for enhancing prognostic outcomes[3]. One of the most destructive characteristics of ICH is its propensity for hematoma expansion (HE), which typically occurs within 6 h after symptom onset and is strongly associated with early clinical deterioration and adverse outcomes. Research has demonstrated that for every 3 ml increase in hematoma volume, the risk of mortality or severe disability approximately increases threefold[4]. In recent years, the blend sign as detected on non contrast-enhanced computed tomography(NCCT) has been recognized as a predictive marker for HE and secondary neurological worsening. The blend sign is characterized by a heterogeneous hematoma comprising regions of hyper-density and hypo-density, with a difference of at least 18 Hounsfield units between the two components[5]. However, the pathologies reflected

[1]Emergency Department, The Affiliated Hospital of Guizhou Medical University, Guiyang 550004, Guizhou Province, People's Republic of China. [2]Laboratory of Emergency Medicine, The Affiliated Hospital of Guizhou Medical University, Guiyang, China. [3]Key Laboratory of Acute Brain Injury and Brain Function Repair in Guiyang, Guizhou Medical University, Guiyang 550004, China. [4]Qian Wu and Lei Huang contributed equally to this work. ✉email: 769070308@qq.com

by these heterogeneous subregions remain unclear. While it is widely accepted that hypodensity areas within the blend sign are indicative of fresh, unclotted active bleeding[6,7] our prior research findings contradicted this notion[8]. Furthermore, we found that the blend sign as a time-sensitive biomarker exhibiting dynamic changes within the initial hours following symptom onset[9]. These findings suggest that traditional qualitative assessments may not fully capture the complex dynamic evolution within a hematoma, whereas quantitative analysis has the potential to provide more objective and precise prognostic information.

Unlike earlier research that emphasized qualitative imaging markers, this study introduces a novel quantitative parameter: the difference in mean Hounsfield Unit (HU) values (dHU) between follow-up and baseline CT scans. This measure captures temporal changes in density within heterogeneous hematoma. Using semi-automated segmentation, the method enables three-dimensional quantification of both hyper-density and hypo-density regions. We propose that a greater dHU, reflecting rapid shifts in hematoma density over a short period, indicates either ongoing bleeding or early clot breakdown. Such changes may serve as a strong predictor of poor functional outcomes.

Methods

Study participants

We performed a retrospective analysis of the medical records from patients with ICH treated between January 2018 and July 2024 at a single center. A diagnosis of ICH was made based on a baseline CT scan performed within 1 h of hospitalization. Patients with a heterogeneous hematoma documented on cranial CT within 6 h of symptom onset were included and subsequently underwent a follow-up CT scan at 24 h after symptom onset. Consistent with previous studies, we excluded patients receiving surgical treatment, patients with traumatic cerebral hemorrhage, arteriovenous malformations, or aneurysms, and those treated using anticoagulation or antiplatelet therapy[10]. Furthermore, patients were excluded if they had undergone contrast-enhanced brain CT within 24 h of symptom onset. Secondary neurological deterioration was defined by either ① requirement for early hemicraniectomy according to the American Stroke Association Guidelines or ② a secondary decrease in Glasgow Coma Scale (GCS) of > 3 points within the first 48 h after symptom onset. Functional outcome was evaluated using the modified Rankin Scale (mRS) at 3 months. Outcomes were classified as favorable if mRS score was ≤ 3 and poor if mRS score was > 3 in accordance with previous studies[9,10]. This retrospective study was conducted with the approval of the Ethics Committee of the Affiliated Hospital of Guizhou Medical University. The requirement for informed consent was waived by the committee.

Imaging analysis

All CT scans on admission and during follow-up were acquired using Siemens 64-slice spiral CT equipment with the following scanning parameters: tube voltage of 120 kV, tube current of 250 mA, slice thickness of 3 mm, field of view (FOV) of 220 mm × 220 mm, matrix size of 512 × 512, and pitch of 0.75. The resulting images had an initial voxel size of $0.43 \times 0.43 \times 3.0\ mm^3$. Images were reconstructed using a soft tissue window algorithm. All imaging data were copied from the archived materials of the hospital's radiology department, and all data were saved in DICOM format. Prior to morphometric and density analyses, images were resampled using linear interpolation to standardize pixel dimensions to a cubic size.

Hematoma segmentation was performed using the Insight Segmentation and Registration Toolkit–Segmentation and Analysis Platform (ITK-SNAP) software (version 4.0; Cognitica, Philadelphia, PA, USA)[11]. Two experienced neurologists (each with 7 years of clinical experience) independently evaluated the location of CT hematoma, ventricular hemorrhage, and the presence of the blend sign (Fig. 3A), while blinded to the patients' clinical data. For each scan, a standardized display window (window width = 80 HU, window level = 35 HU) was applied to optimize hematoma visualization. The hematoma was then delineated using a semi-automatic approach with manual refinement to generate a three-dimensional (3D) region of interest (ROI). The average segmentation time was approximately 15 min per scan. From the final 3D ROI, the software automatically calculated the following quantitative features: ① total hematoma volume; ② overall mean hematoma density; ③ mean densities of the hyper-density and hypo-density regions of heterogeneous hematoma[5,12]. The dHU value was determined by subtracting the mean HU value of the entire hematoma at admission from that at follow-up[13]. The complete workflow for image processing and segmentation is illustrated in (Fig. 1), and a representative example of CT slices with the corresponding 3D reconstructed hematoma is shown in (Fig. 2). For this study, hematoma expansion was defined as an absolute increase > 6 ml or a relative increase > 33% on follow-up CT compared with baseline[14].

A shows the whole hematoma segmentation, B shows the subsegmentation into hyper-density and hypo-density regions, and E–F show their corresponding 3D reconstructions. C–D highlight the hyper- and hypo-density regions separately, and G–H display the 3D visualization models, where blue indicates the overall hematoma with a mean density of 67 ± 14 HU, red indicates the hyper-density area with a mean density of 72 ± 12 HU, and green indicates the hypo-density area with a mean density of 46 ± 8 HU.

Statistical analyses

All statistical analyses were performed using SPSS software (version 26.0; IBM Corporation, Armonk, NY). Continuous variables are reported as either the mean ± standard deviation if normally distributed or median [interquartile range] if non-normally distributed, with normality assessed using the Shapiro–Wilk test. Normally distributed variables were compared by Student's t-test and non-normally distributed variables by Mann-Whitney U-test. A *P*-value less than 0.05 (two-tailed) was deemed statistically significant for all tests. Categorical variables are presented as percentages and analyzed using chi-square or Fisher's exact test. We conducted univariate analysis to identify variables significantly linked to HE and poor clinical outcomes. Variables with p-values < 0.05 were further evaluated using multivariable logistic regression to determine their

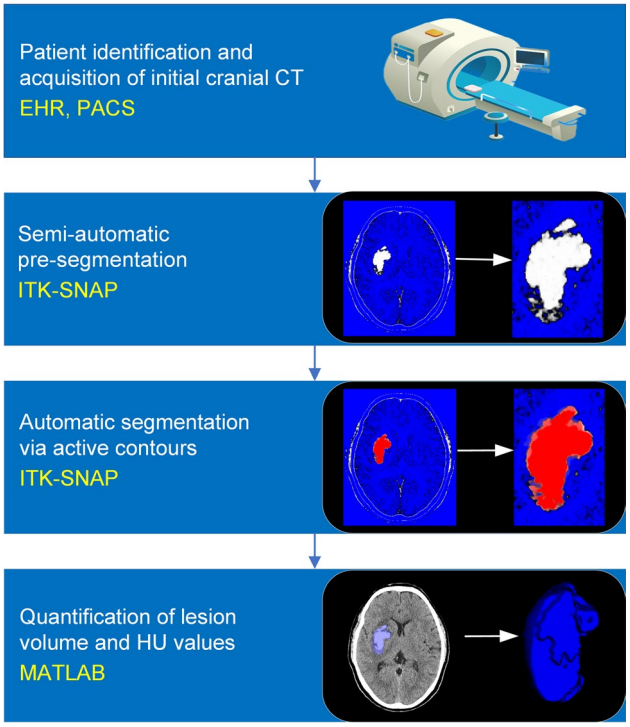

Fig. 1. Image processing flowchart displaying data collection, pre-processing, segmentation and information extraction. (Yellow text denotes software libraries; EHR = Electronic Health Record; PACS = Picture Archiving and Communication System; ITK-SNAP = The Insight Toolkit Segmentation and Registration Platform).

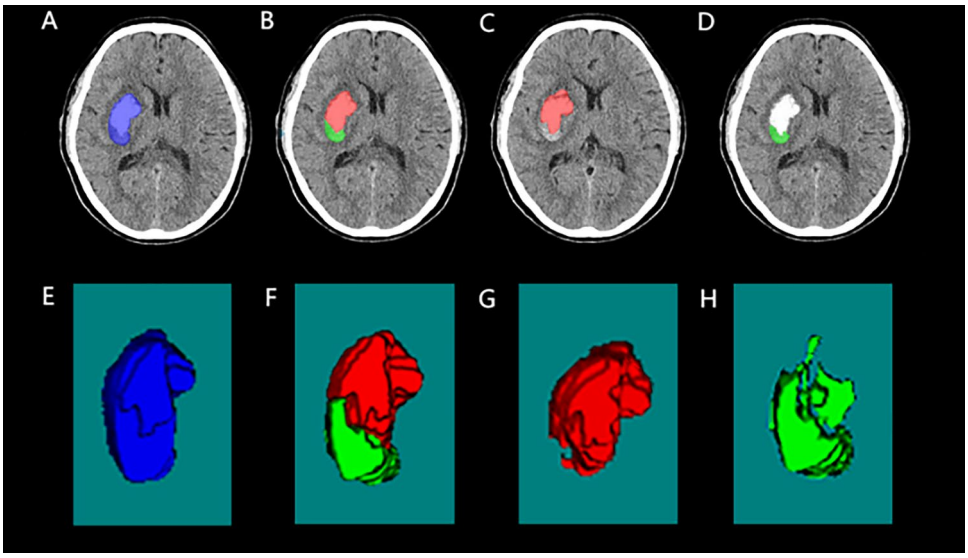

Fig. 2. Examples of heterogeneous hematoma segmentation illustrated with ITK-SNAP.

independent association with these outcomes. To assess and reduce potential multicollinearity among predictors, variance inflation factors (VIFs) were examined[15]. Factors with a VIF greater than 5 and tolerance less than 0.1 were systematically excluded to refine the model structure and minimize potential parameter estimation bias. Subsequently, multivariate regression analysis was performed to identify the independent predictors of adverse outcomes. The interobserver reliability of the heterogeneous hematoma was assessed by calculating Cohen's kappa (κ) values, based on the criteria established in a previous study[9].

Results

Baseline characteristics of the study cohort

A total of 261 patients (198 males and 63 females, median age 55.0 years, IQR [48.0–64.0]) with confirmed heterogeneous hematoma on CT images were included in this study according to preset inclusion and exclusion criteria. Baseline GCS score was 13.0 [10.0–14.0] and initial average hematoma volume was 29.0 mL [17.0–42.0]. The mean difference in volume-averaged CT value at follow-up compared to the initial condition (dHU) for all patients was 0.715 ± 6.365 HU. A total of 72 patients (28%) experienced HE. Poor outcomes were evaluated as follows: secondary neurological deterioration within 48 h (69 patients, 26%); 30-day mortality (21 patients, 8%); and 3-month poor mRS (4–6) (102 patients, 39%) (Supplementary Table S1). Notably, the incidence of hematoma enlargement was significantly higher in patients with dHU > 3.25 than in those with dHU ≤ 3.25 (43% vs. 27%, $P = 0.017$) (Table 1). Mean dHU was significantly greater (i.e., the increase in density at follow-up was larger) among patients with secondary neurological deterioration within 48 h of baseline CT acquisition (OR = 1.111, 95%CI 1.056–1.168, $P < 0.001$), 30-day mortality (OR = 1.061, 95%CI 1.028–1.102, $P = 0.018$), and poor mRS (4–6) 3 months after ICH (OR = 1.059, 95%CI 1.016–1.104, $P = 0.007$) (Table 2 and Supplementary Table S2).

ROC analysis results for distinguishing outcomes according to dHU

A ROC curve was constructed to define a dHU cutoff value optimal for distinguishing good from poor prognosis (mRS > 3). This analysis yielded a cutoff of 3.25 HU (area under the ROC curve [AUC] = 0.707, 95%CI 0.646–0.769, $P < 0.001$) (Fig. 3B), and dHU > 3.25 HU predicted poor outcome with 48.2% sensitivity, 89.7% specificity, 88.7% positive predictive value, and 50.6% negative predictive value. The distribution of mRS at 90 days in patients with dHU > 3.25 and those without is shown in (Fig. 3C).

Characteristics	dHU ≤ 3.25 ($n = 172$)	dHU > 3.25 ($n = 89$)	*P* value
Age, median [IQR]	55. 0 [48.0,64.8]	56.0 [49.5,64.0]	0.725
Gender, male (%)	131 (76)	67 (75)	0.875
Hypertension, n (%)	119 (69)	61 (69)	0.141
Diabetes mellitus, n (%)	16 (9)	4 (4)	0.166
SBP (mmHg)	164.5 [145.0,186.8]	171.0 [154.5,190.5]	0.084
DBP (mmHg)	98.0 [88.0,111.8]	103.0 [89.0,118.0]	0.111
Time from onset to baseline CT (h)	4.5 [2.5,4.9]	2.6 [2.0,3.7]	<0.001
Time from baseline CT to follow-up CT (h)	9.6 [8.0,11.7]	8.9 [7.7,10.6]	0.031
GCS on admission	13.0 [11.0,14.0]	12.0 [10.0,14.0]	0.096
Laboratory testing			
WBC (10^9/L)	8.9 [6.4,11.6]	8.9 [7.5,10.9]	0.632
RBC (10^9/L)	4.8 [4.3,5.2]	4.8 [4.4,5.3]	0.721
Hb (g/L)	144.8 ± 18.8	146.1 ± 17.7	0.610
Platelet count (10^9/L)	202.0 [155.3,242.5]	189.0 [154.5,229.0]	0.367
APTT (s)	33.4 [30.9,36.6]	33.4 [30.8,35.4]	0.426
PT (s)	12.7 [12.2,13.3]	12.8 [12.1,13.2]	0.908
Fibrinogen (g/L)	2.7 [2.4,3.2]	2.7 [2.4,3.2]	0.773
INR	0.9 [0.9,1.0]	0.9 [0.9,1.0]	0.935
Radiographic status			
Deep, n (%)	116 (67)	68 (76)	0.460
Lobar, n (%)	48 (27)	19 (21)	0.341
Infratentorial, n (%)	8 (5)	2 (2)	0.217
Hematoma volume (mL)	29.0 [17.0,44.5]	29.0 [18.5,40.5]	0.915
HE, n (%)	50 (29)	39 (43)	0.017

Table 1. Comparison of baseline characteristics among ICH patients with dHU > 3.25 or dHU ≤ 3.25.GCS, Glasgow coma scale; SBP, systolic blood pressure; DBP, diastolic blood pressure; WBC, white blood cell count; RBC, red blood cell count; Hb, hemoglobin; APTT, Activated partial thromboplastin time; PT, prothrombin time; INR, international normalized ratio; HE: hematoma expansion.

The dHU value for predicting secondary neurological deterioration

Univariate analysis found significant differences in GCS score ($P = 0.001$), hematoma volume ($P < 0.001$), SBP ($P = 0.006$), DBP ($P = 0.002$), whole hematoma mean HU at follow up ($P = 0.003$), hyper-area CT value during follow-up ($P = 0.001$), and dHU value ($P < 0.001$) for secondary neurological deterioration in 48 h (Table 2). Subsequently, multivariate logistic regression analysis revealed that larger baseline hematoma volume (OR: 1.090; 95% CI: 1.057–1.123; $P < 0.001$); lower GCS score (OR: 0.832; 95% CI: 0.711–0.974; $P = 0.022$); and larger dHU value (OR: 1.116; 95% CI: 1.031–1.208; $P = 0.006$) were independently associated with secondary neurological deterioration in 48 h (Table 2).

Characteristics	Secondary neurological deterioration within 48 h			Poor 3-month mRS score		
	OR	95%CI	*P*-value	OR	95%CI	*P*-value
Age	1.001	0.979–1.023	0.953	1.011	0.991–1.031	0.301
Gender	1.109	0.580–2.120	0.754	1.345	0.746–2.426	0.325
Hypertension	1.116	0.628–1.984	0.708	1.330	0.790–2.240	0.283
Diabetes mellitus	0.661	0.252–1.731	0.399	1.273	0.490–3.304	0.620
SBP	1.015	1.004–1.026	0.006	1.009	1.000–1.018	0.063
DBP	1.025	1.009–1.041	0.002	1.015	1.002–1.028	0.028
Clinical/radiographic status at admission						
Time from onset to baseline CT	0.998	0.997–1.001	0.513	0.997	0.989–1.004	0.375
Time from baseline CT to follow-up CT	0.820	0.512–1.300	0.397	0.859	0.483–1.527	0.601
GCS on admission	0.812	0.716–0.920	0.001	0.620	0.752–0.924	0.001
Hematoma volume	1.093	1.063–1.125	0.000	1.037	1.020–1.055	0.000
Laboratory testing						
WBC	1.071	0.990–1.159	0.087	1.078	1.006–1.156	0.032
RBC	1.157	0.776–1.723	0.474	1.014	0.711–1.447	0.937
Hb	1.004	0.989–1.019	0.596	1.002	0.988–1.015	0.795
Platelet count	0.999	0.995–1.003	0.734	0.998	0.995–1.002	0.431
APTT	0.941	0.884–1.002	0.056	0.996	0.941–1.053	0.883
INR	0.389	0.039–3.862	0.420	2.584	0.973–1.033	0.142
PT	0.420	0.757–1.146	0.500	0.976	0.920–1.035	0.417
Fibrinogen	1.373	0.951–1.982	0.090	1.058	0.884–1.268	0.538
Radiographic status						
Deep	0.713	0.479–1.035	0.094	1.136	0.942–2.590	0.084
Lobar	1.065	0.188–6.027	0.943	0.295	0.570–1.529	0.146
Infratentorial	1.816	0.136–4.890	0.824	0.220	0.038–1.270	0.090
Baseline CT, mean HU						
Whole hematoma	0.955	0.904–1.008	0.096	0.950	0.904–0.998	0.042
hypo-area	0.973	0.935–1.012	0.172	0.990	0.955–1.025	0.561
hyper-area	0.958	0.905–1.013	0.131	0.912	0.864–0.962	0.001
Difference between hypo and hyper area	1.007	0.966–1.050	0.741	0.963	0.927–1.000	0.053
Follow-up CT, mean HU						
whole hematoma	1.074	1.024–1.127	0.003	1.024	0.983–1.067	0.258
hypo-area	1.034	1.001–1.069	0.051	1.016	0.986–1.046	0.304
hyper-area	1.097	1.040–1.156	0.001	1.021	0.977–1.067	0.364
Difference between hypo and hyper area	1.008	0.972–1.046	0.653	0.992	0.960–1.025	0.637
dHU	1.111	1.056–1.168	0.000	1.059	1.016–1.104	0.007
Multivariate analysis						
Hematoma volume	1.090	1.057–1.123	0.000	1.019	1.001–1.037	0.040
GCS	0.832	0.711–0.974	0.022	0.784	0.682–0.901	0.001
SBP	1.004	0.986–1.021	0.669	-	-	-
DBP	1.017	0.991–1.044	0.196	1.017	1.000–1.035	0.053
HU of whole hematoma (initial CT)	-	-	-	1.118	1.012–1.234	0.028
HU of hyper-area (initial CT)	-	-	-	0.839	0.756–0.930	0.001
HU of whole hematoma (follow-up CT)	0.948	0.856–1.049	0.298	-	-	-
HU of hyper-area (follow-up CT)	1.068	0.962–1.187	0.218	-	-	-
dHU	1.116	1.031–1.208	0.006	1.156	1.086–1.232	0.000

Table 2. Independent associations of dHU with poor outcomes. GCS, Glasgow coma scale; SBP, systolic blood pressure; DBP, diastolic blood pressure; WBC, white blood cell count; RBC, red blood cell count; Hb, hemoglobin; APTT, Activated partial thromboplastin time; PT, prothrombin time; INR, international normalized ratio; Hounsfield unit, HU; dHU = difference of mean HU.

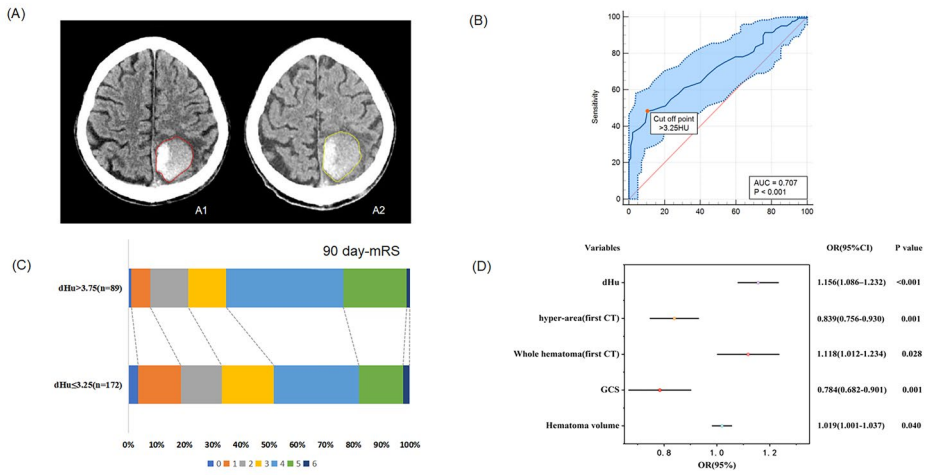

Fig. 3. Illustration of the analytic procedures and results. (**A**) Example blend sign segmentation results using ITK-SNAP. A1 refers to the cranial CT scan images performed from symptom onset to hospital admission, A2 indicates the follow-up cranial CT scans conducted within 24 h after admission. (**B**) Receiver operating characteristic (ROC) curves of dHU for predicting poor outcome. (**C**) 90-Day mRS scores for ICH patients with dHU > 3.25 and ≤ 3.25. (**D**) Multivariable analysis for the associations between dHU and poor outcomes.

Independent association of dHU value with poor outcomes

Baseline GCS score, initial hematoma volume, and dHU value were significantly associated with 30-day mortality and unfavorable 3-month mRS scores (4–6) by univariate analysis (all $P < 0.05$). Adjusted multivariate logistic regression models demonstrated that elevated dHU values were independently associated with adverse clinical outcomes. Specifically, each unit increase in dHU conferred 15.6% higher odds of unfavorable functional recovery at 3-month follow-up (OR: 1.156; 95% CI: 1.086–1.232; $P < 0.001$), with a distinct dose-response relationship visualized in (Fig. 3D). Although the association with 30-day mortality showed similar directional trends (OR: 1.090; 95% CI 1.025–1.150; $P = 0.023$)(Supplementary Table S2). Additionally, the dHU value demonstrated a significant correlation with secondary neurological outcomes, 30-day mortality, and poor mRS at three months within the context of a VIF logistic regression model (Supplementary Table S3).

Discussion

Our present study showed the existence of an association between the hyper-dense region of a heterogeneous hematoma and neurological deficits in ICH patients, with increasing dHU indicating greater hematoma instability linked to poor prognosis. Specifically, we report that a mean increase of > 3.25 HU at follow-up relative to baseline is predictive of poor prognosis. After adjusting for established prognostic factors, each 1 HU increase in dHU was associated with a 12% higher likelihood of secondary neurological deterioration and a 16% higher likelihood of poor functional outcomes. This quantitative metric offers an improvement over static imaging features by capturing the dynamic instability of the hematoma, which may contribute to secondary brain injury through mechanisms such as hematoma expansion.

Rapidly increasing hematoma density is associated with poorer clinical outcomes, and the underlying pathophysiological mechanisms are complex. Although the natural evolution of a stable blood clot may lead to a physiological increase in density due to clot retraction and serum exudation[16] our findings suggest that in certain unstable hematoma, this process is pathologically intensified. The rapid or abnormal density increase captured by high dHU values may not reflect benign clot maturation, but rather could result from ongoing microhemorrhage, active extravasation of plasma proteins into the clot, and abnormal remodeling of the fibrin network[17]. Recent studies have further confirmed that dHU > 2.5 HU independently predicts poor functional outcomes at 90 days, supporting its potential as a marker of hematoma instability[13]. This short-term change in hematoma CT attenuation reflects a metabolically active and unstable hematoma, which may exacerbate perihematomal edema and neurotoxicity[18,19]. Our data corroborate this observation: among patients with dHU > 3.25, the incidence of HE was significantly higher (43% vs. 27%; $P = 0.017$), directly linking this dynamic density change to a well-established mechanism of secondary brain injury.

Another important finding of our analysis is the differing prognostic significance of hyper-density and hypo-density regions within a heterogeneous hematoma. Using semi-automated segmentation, our analysis indicated a possible trend in which the HU of the hyper-density area on initial CT was more strongly associated with poor clinical outcomes, whereas such an association was not evident for the surrounding hypo-density region. This supports the view that the hyper-density area seen in the CT blend sign is closely associated with active pathological processes. Previous research has shown that in patients with both the CT blend sign and the CT angiography spot sign, which is a direct imaging marker of ongoing bleeding, the spot sign was located within the hyper-density region in up to 92.7% of cases[20,21]. This observation supports the hypothesis that the hyper-density area constitutes the primary pathological focus within heterogeneous hematoma[8]. Our findings

therefore provide imaging evidence that can guide more precise and less invasive surgical strategies. In planning interventions such as catheter or endoscopic evacuation, priority should be given to accessing and removing the unstable hyper-density core. Targeting this region may be more effective in preventing hematoma expansion and improving patient outcomes.

In addition to the aforementioned imaging findings, this study also confirms the prognostic significance of key clinical factors. Lower GCS scores and larger initial hematoma volumes upon admission are robust predictors of both long-term poor outcomes and secondary neurological deterioration within 48 h in patients with ICH. This conclusion aligns closely with a substantial body of existing literature[22–24]. These two variables constitute the foundational components of classical ICH scoring systems, and their role as independent prognostic factors has been consistently supported by prior research.

In our cohort, 76% of patients were male. Although this proportion is higher than that reported in some general population studies, it is consistent with established epidemiological trends for ICH[25]. The higher incidence of ICH in males is well documented, particularly among Asian populations. For example, large-scale clinical trials conducted in China, including the CARICH and E-start studies, reported that approximately 72% of patients were male[26,27]. The close concordance between our findings and those from previous large cohorts supports the representativeness of our study population. This validation provides a robust basis for further evaluating the incremental prognostic value of the novel imaging marker dHU in addition to conventional prognostic factors.

While dHU demonstrates potential for ICH prognosis assessment, several limitations must be acknowledged. First, our single-center cohort may introduce selection bias. Moreover, the generalizability of dHU thresholds across diverse ICH populations requires validation through multi-institutional studies. Furthermore, our semi-automated segmentation method requires specialized software and technical expertise, which may limit its immediate adoption in clinical settings. Future research should prioritize the development of fully automated, machine learning-based algorithms to improve accessibility and facilitate broader clinical implementation. Beyond dHU, we suggest investigating the timing and density gradients between hyper- and hypo-density regions within hematoma as a complementary parameter. These analyses may improve our understanding of hematoma architecture's impact on clinical outcomes and guide stratified treatment for ICH patients.

Conclusion

In summary, this study introduces a novel and clinically relevant approach for assessing heterogeneous hematoma through the application of the ITK-SNAP tool, which supports semi-automatic segmentation and enables accurate quantitative evaluation of density variations within hematoma. By introducing the concept of dHU, we identified a threshold value of 3.25 dHU, which shows significant predictive potential for poor clinical outcomes. Our findings suggest that hyper-density region within heterogeneous hematoma may represent the primary pathological substrate contributing to neurological deterioration. Accordingly, this study highlights the clinical importance of preventing hematoma density escalation as a key therapeutic objective, which may play a critical role in improving outcomes for patients with acute heterogeneous hematoma.

Data availability

The raw data supporting the conclusions of this article will be made available by the corresponding author, Likun Wang (769070308@qq.com), upon reasonable request.

Received: 23 March 2025; Accepted: 1 September 2025
Published online: 26 September 2025

References

1. Li, L. et al. Risks of recurrent stroke and all serious vascular events after spontaneous intracerebral haemorrhage: pooled analyses of two population-based studies. *Lancet Neurol.* **20**, 437–447. https://doi.org/10.1016/s1474-4422(21)00075-2 (2021).
2. Querfurth, H., Marczak, I., Rahimian, N. & Jijakli, A. Green-LaRoche, D. Spontaneous intracranial hemorrhages in a community of Asian americans: case series and literature review. *Cureus* **16**, e52128. https://doi.org/10.7759/cureus.52128 (2024).
3. Sheth, K. N. Spontaneous intracerebral hemorrhage. *N Engl. J. Med.* **387**, 1589–1596. https://doi.org/10.1056/NEJMra2201449 (2022).
4. Puy, L., Boe, N. J., Maillard, M., Kuchcinski, G. & Cordonnier, C. Recent and future advances in intracerebral hemorrhage. *J. Neurol. Sci.* **467**, 123329. https://doi.org/10.1016/j.jns.2024.123329 (2024).
5. Wu, Q., Chen, N., Wu, G. & Wang, L. Integrative mechanistic insights and clinical implications of the blend sign in intracerebral hemorrhage. *Neuroscience* **583**, 43–52. https://doi.org/10.1016/j.neuroscience.2025.07.040 (2025).
6. Wang, W., Zhou, N. & Wang, C. Early-Stage estimated value of blend sign on the prognosis of patients with intracerebral hemorrhage. *Biomed. Res. Int.* **2018** (4509873). https://doi.org/10.1155/2018/4509873 (2018).
7. Li, Q. et al. Blend sign on computed tomography: novel and reliable predictor for early hematoma growth in patients with intracerebral hemorrhage. *Stroke* **46**, 2119–2123. https://doi.org/10.1161/strokeaha.115.009185 (2015).
8. Li, Y. et al. Is the CT blend sign composed of two parts of blood with different age?? *Neurocrit Care.* **35**, 367–378. https://doi.org/10.1007/s12028-020-01165-1 (2021).
9. Wu, Q. et al. Morphological characteristics of CT blend sign predict hematoma expansion and outcomes in intracerebral hemorrhage in elderly patients. *Front. Med. (Lausanne).* **11**, 1442724. https://doi.org/10.3389/fmed.2024.1442724 (2024).
10. Wu, G. et al. Post-operative re-bleeding in patients with hypertensive ICH is closely associated with the CT blend sign. *BMC Neurol.* **17** https://doi.org/10.1186/s12883-017-0910-6 (2017).
11. Yushkevich, P. A., Yang, G. & Gerig, G. ITK-SNAP: an interactive tool for semi-automatic segmentation of multi-modality biomedical images. *Annu. Int. Conf. IEEE Eng. Med. Biol. Soc.* **2016**, 3342–3345. https://doi.org/10.1109/embc.2016.7591443 (2016).
12. Street, J. S., Pandit, A. S. & Toma, A. K. Predicting vasospasm risk using first presentation aneurysmal subarachnoid hemorrhage volume: A semi-automated CT image segmentation analysis using ITK-SNAP. *PLoS One.* **18**, e0286485. https://doi.org/10.1371/journal.pone.0286485 (2023).

13. Xia, X. et al. Difference of mean Hounsfield units (dHU) between follow-up and initial Noncontrast CT scan predicts 90-day poor outcome in spontaneous supratentorial acute intracerebral hemorrhage with deep convolutional neural networks. *Neuroimage Clin.* **38**, 103378. https://doi.org/10.1016/j.nicl.2023.103378 (2023).
14. Morotti, A. et al. Non-contrast CT markers of intracerebral hemorrhage expansion: the influence of onset-to-CT time. *Int. J. Stroke.* **18**, 704–711. https://doi.org/10.1177/17474930221142742 (2023).
15. Kim, J. H. Multicollinearity and misleading statistical results. *Korean J. Anesthesiol.* **72**, 558–569. https://doi.org/10.4097/kja.19087 (2019).
16. Cines, D. B. et al. Clot contraction: compression of erythrocytes into tightly packed polyhedra and redistribution of platelets and fibrin. *Blood* **123**, 1596–1603. https://doi.org/10.1182/blood-2013-08-523860 (2014).
17. Yassi, N. et al. Tranexamic acid for intracerebral haemorrhage within 2 hours of onset: protocol of a phase II randomised placebo-controlled double-blind multicentre trial. *Stroke Vasc Neurol.* **7**, 158–165. https://doi.org/10.1136/svn-2021-001070 (2022).
18. Kim, Y. S. et al. Mediation effects of mean Hounsfield unit on relationship between hemoglobin and expansion of intracerebral hemorrhage. *Sci. Rep.* **11**, 17236. https://doi.org/10.1038/s41598-021-96790-x (2021).
19. Jeong, H. G., Bang, J. S., Kim, B. J., Bae, H. J. & Han, M. K. Hematoma Hounsfield units and expansion of intracerebral hemorrhage: A potential marker of hemostatic clot contraction. *Int. J. Stroke.* **16**, 163–171. https://doi.org/10.1177/1747493019895703 (2021).
20. Wu, Q. et al. Is the hyperdensity areas of the CT blend sign associated with the fresh bleeding in intracerebral hemorrhage?? *Curr. Med. Imaging.* **20**, e15734056310498. https://doi.org/10.2174/0115734056310498241017052529 (2024).
21. Wada, R. et al. CT angiography spot sign predicts hematoma expansion in acute intracerebral hemorrhage. *Stroke* **38**, 1257–1262. https://doi.org/10.1161/01.STR.0000259633.59404.f3 (2007).
22. Hemphill, J. C. 3, Bonovich, D. C., Besmertis, L., Manley, G. T., Johnston, S. C. & rd,, & The ICH score: a simple, reliable grading scale for intracerebral hemorrhage. *Stroke* **32**, 891–897. https://doi.org/10.1161/01.str.32.4.891 (2001).
23. Lord, A. S., Gilmore, E., Choi, H. A. & Mayer, S. A. Time course and predictors of neurological deterioration after intracerebral hemorrhage. *Stroke* **46**, 647–652. https://doi.org/10.1161/strokeaha.114.007704 (2015).
24. Morotti, A. et al. Association between hematoma expansion severity and outcome and its interaction with baseline intracerebral hemorrhage volume. *Neurology* **101**, e1606–e1613. https://doi.org/10.1212/wnl.0000000000207728 (2023).
25. Schrag, M. & Kirshner, H. Management of intracerebral hemorrhage: JACC focus seminar. *J. Am. Coll. Cardiol.* **75**, 1819–1831. https://doi.org/10.1016/j.jacc.2019.10.066 (2020).
26. Zhang, C. et al. Clot removal with or without decompressive craniectomy under ICP monitoring for supratentorial intracerebral hemorrhage (CARICH): a randomized controlled trial. *Int. J. Surg.* **110**, 4804–4809. https://doi.org/10.1097/js9.0000000000001466 (2024).
27. Liu, Q. et al. Safety and efficacy of early versus delayed acetylsalicylic acid after surgery for spontaneous intracerebral haemorrhage in China (E-start): a prospective, multicentre, open-label, blinded-endpoint, randomised trial. *Lancet Neurol.* **23**, 1195–1204. https://doi.org/10.1016/s1474-4422(24)00424-1 (2024).

Acknowledgements

We thank LetPub for its linguistic assistance during the preparation of this manuscript.

Author contributions

QW: Conceptualization, Writing—original draft. LH: Data curation, Project administration. NC: Software, Writing—original draft. SR: Investigation, Writing—review & editing. FY: Methodology. XZ: Project administration. GW: Resources, Writing—review & editing. LW: Supervision, Methodology, Writing—review & editing.

Funding

The author(s) declare that financial support was received for the research, authorship, and/or publication of this article. This research received support from the Natural Science Foundation of China (82260244), The Leading Discipline Program of the Affiliated Hospital of Guizhou Medical University (gyfyxkrc-2023–05). Key laboratory of Guizhou Medical University [2024] fy007. Supported the Key Advantageous Discipline Construction Project of Guizhou Provincial Health Commission in 2023 in Emergency Department.

Declarations

Competing interests

The authors declare no competing interests.

Ethics statement

The study was conducted in accordance with the Declaration of Helsinki, and the protocol was approved by the Ethics Committee of the Affiliated Hospital of Guizhou Medical University (Approval No. 2019/114). The committee waived the requirement for informed consent due to the retrospective nature of the study and the use of de-identified data.

Additional information

Supplementary Information The online version contains supplementary material available at https://doi.org/10.1038/s41598-025-18409-9.

Correspondence and requests for materials should be addressed to L.W.